JOURNAL OF CHEMICAL & ENGINEERING DATA

Article

pubs.acs.org/jced

# Adsorption Modeling with Soret-Like and Dufour Effects of a Two-Component Organic Gas on Activated Carbon

Liqing Li,* Zheng Liu, Jundong Xin, Jianfei Song, and Lin Tang

School of Energy Science and Engineering, Central South University, Changsha 410083, China

**ABSTRACT:** Adsorption of a two-component gas mixture of acetone and methylbenzene was tested in a fixed-bed apparatus, and a coupled model of heat and mass transfer was developed according to the theory of Soret and Dufour effects. The numerical simulation results agreed well with the experimental results. Using this mathematical model, the coupled effects of heat and mass transfer were studied in a fixed-bed adsorption simulation, and numerical analysis results were used to discuss the influences of heat transfer coefficients, mass transfer coefficients, and the coupled effect of heat and mass transfer on the fixed-bed process. These results show that heat transfer coefficients have little effect on mass transfer. In contrast, mass transfer coefficients have some impact on heat transfer. The mass transfer effect caused by the temperature gradient is more obvious than the heat transfer effect caused by the concentration gradient.

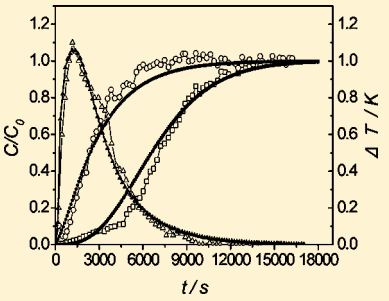


## INTRODUCTION

Activated carbon, an excellent adsorbent and a versatile technology, has been used successfully to control emissions of volatile organic compounds (VOCs), and its properties have been well-studied.[1−4] Meanwhile, Soret and Dufour were the first to propose the existence of a coupling effect between heat and mass transfer in porous media, such as activated carbon. The Soret effect, also referred to as the thermal diffusion effect, refers to mass transfer caused by a temperature gradient. The Dufour effect, or the diffusion thermal, is the reciprocal phenomenon; it describes the heat flux caused by a concentration gradient. Martynenko and Pavlyukevich[5] provide a detailed introduction to heat and mass transfer processes in porous media. Malashetty and Gaikwad[6] investigated the effect of cross diffusion, namely, the role of the Soret and Dufour coefficients on double diffusive convection in an unbounded, vertically stratified two-component system. Cheng[7] studied the effects of the Soret and Dufour parameters on coupled heat and mass transfer by natural convection from a vertical truncated cone in a porous medium. Postelnicu[8] and Coelho and Telles[9] demonstrated that the influence of the coupling effect between heat and mass transfer in the adsorption process can be significant, especially when large concentration and temperature gradients exist or when components in a mixture have considerably different molecular weights. But research on coupled diffusion from heat and mass transfer interactions in the adsorption process is lacking.

To address this research gap, we studied a fixed-bed adsorptive purification experiment, developed a coupled mathematical model of heat and mass transfer interactions in the adsorption process, and compared the results from simulations and experiments. The mathematical model used numerical analysis to simulate fixed-bed adsorption and the coupled effect of heat and mass transfer. With this mathematical model and Athena Visual Studio, we simulated the adsorption of a methylbenzene and acetone gas mixture in a fixed bed of activated carbon.

## EXPERIMENTAL SYSTEM

Columnar activated carbon (JinJun Long Carbon Industry Chemical Ltd. Co., Guangzhou, China), the physical properties of which are shown in Table 1, was used as the adsorbent in this study. A mixture of acetone and methylbenzene (Koster and Bohmke Ltd., Germany, with a purity of greater than 99.5 %, respectively), was used as the adsorbate.

**Table 1. Parameters of Activated Carbon**

| parameter | value |
|---|---|
| total pore volume/$cm^3 \cdot g^{-1}$ | 0.1545 |
| micropore volume/$cm^3 \cdot g^{-1}$ | 0.1007 |
| mesopore volume/$cm^3 \cdot g^{-1}$ | 0.0347 |
| macropore volume/$cm^3 \cdot g^{-1}$ | 0.0191 |
| BET surface area/$m^2 \cdot g^{-1}$ | 237.4 |
| actual density/$10^3$ $kg \cdot m^{-3}$ | 2.2 |
| packed density/$10^3$ $kg \cdot m^{-3}$ | 0.88 |
| ash/% | 1.5 |
| porosity/% | 61.5 |
| particle size/mm | 3.5−4 |

A fixed adsorption bed experiment was used to study the adsorption process. The experimental apparatus, shown in Figure 1, consisted of a gas distribution system, a constant temperature system (thermostatic water tank, DC1015, China), a fixed-bed adsorption column (filled to a length of 0.45 m, diameter $D$ = 0.0028 m), and a manufactured test system (GC FID, RS53-T, Germany). In the experiment, a micropump repeatedly sprayed organic solvents through a constant temperature zone to form

**Received:** October 26, 2011
**Accepted:** December 7, 2011
**Published:** December 23, 2011

  

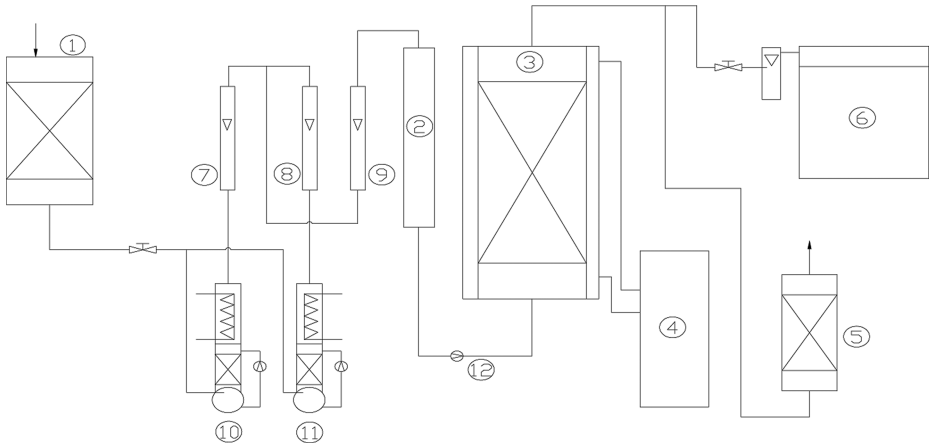


**Figure 1.** Experimental apparatus for adsorption. Symbols: 1, air drying column; 2, gas mixing column; 3, fixed bed; 4, thermostatic water tank; 5, adsorption column for exhaust gas treatment; 6, gas chromatograph; 7, methylbenzene flowmeter; 8, acetone flowmeter; 9, mixed gas flowmeter; 10, methylbenzene generator; 11, acetone generator; 12, vacuum pump.

saturated organic steam. This saturated steam was then mixed with dry air to achieve the desired concentration of organic gas. The mixed gas was vacuum pumped into the fixed adsorption bed, where it was adsorbed by activated carbon. Finally, the gas was purified and discharged. The adsorption process was assumed to be in an equilibrium state when the concentrations of acetone and methylbenzene in the discharge gas equaled that of the inlet gas for 30 min or more. The inlet and outlet concentrations of methylbenzene and acetone in experiment are measured by gas chromatography.

## MATHEMATICAL MODEL

**Assumptions.** To develop the mathematical model, a simplified version of the actual adsorption processes with several assumptions was considered.[10−14] The assumptions included the following:

(1) The gas was assumed to be ideal with stable flow, components, and temperature.
(2) The adsorption of air by activated carbon was neglected.
(3) To simplify the adsorption process, the gas velocity along the axis of the adsorption bed was constant, and the gas flow rate, pressure, and component concentration degree along with the radial gradient of adsorption bed were ignored.
(4) The axial diffusion piston flow model was used for the gas phase flow.
(5) Adsorption heat was to be considered, and the gas−solid phase was assumed to reach thermal equilibrium instantaneously, because the time of collision gas−solid is much less than the transfer time in bed.
(6) The effects of heat and mass transfer were assumed to be coupled.

**Model Development.** With the above assumptions, the problem was simplified to a one-dimensional, nonisothermal model. The governing equation of the adsorption purification process is given below.

**Gas-Phase Mass Equilibrium Equation.** The model[15] used for mass transfer in the gas phase is given below:

$$-D_{ax}\frac{\partial^2 C_i}{\partial z^2} + v\frac{\partial C_i}{\partial z} + \frac{\partial C_i}{\partial t} + \rho_p\left(\frac{1-\varepsilon}{\varepsilon}\right)\frac{\partial q_i}{\partial t} = 0 \quad (1)$$

where $D_{ax}$ is the axial diffusion coefficient, $v$ is the empty column gas velocity, $\varepsilon$ is the adsorbent porosity, $z$ is the bed's axial coordinates; $\rho_p$ is the adsorbent packing density, $q$ is the solid-phase concentration, and $t$ is the adsorption time.

Adsorbed gases meet the ideal gas assumption, namely, $C_i = (Py_iM_i/RT)$. Here $C_i$ is the concentration of component $i$, kg·m$^{-3}$; $y_i$ is the mole fraction of component $i$; $M_i$ is the molar mass of component $i$, kg·mol$^{-1}$; $R_g$ is the gas constant, J·mol$^{-1}$·K$^{-1}$; $T$ is the gas temperature in the column, and $P$ is the column's internal pressure.

Inserting these terms into eq 1 gives the following equation:

$$-D_{ax}\frac{\partial^2 y_i}{\partial z^2} + v\frac{\partial y_i}{\partial z} + \frac{\partial y_i}{\partial t} + \rho_p\left(\frac{1-\varepsilon}{\varepsilon}\right)\frac{R_gT}{PM_i}\frac{\partial q_i}{\partial t} = 0 \quad (2)$$

**Energy Conservation Equation.** Assuming temperature allows instantaneous equilibrium between the solid and gas phases, the equation[15] for energy conservation becomes the following:

$$-K_L\frac{\partial^2 T}{\partial z^2} + \varepsilon\rho_g c_{pg} v\frac{\partial T}{\partial z} + (\varepsilon\rho_g c_{pg} + \rho_p c_{ps})\frac{\partial T}{\partial t} - \rho_p\sum_{i=1}^{n}(-\Delta H_i)\frac{\partial q_i}{\partial t} + \frac{2h_i}{r_{Bi}}(T - T_w) = 0 \quad (3)$$

where $K_L$ is the thermal axial dispersion coefficient, $c_{pg}$ is the column gas heat capacity, J·mol$^{-1}$·K$^{-1}$; $c_{ps}$ is the solid-phase adsorbent heat capacity, J·kg$^{-1}$·K$^{-1}$; $\rho_p$ is the true bed density, $\rho_g$ is the column gas density, and $\Delta H$ is the equivalent heat adsorption, J·mol$^{-1}$.

Neglecting wall heat transfer in axial dispersion, the energy equation to calculate the bed boundary energy is given below:

$$\rho_w c_{pw} A_w\frac{\partial T_w}{\partial t} = 2\pi r_{Bi}h_i(T - T_w) - 2\pi r_{Bo}h_o(T_w - T_{atm}) \quad (4)$$

$$A_w = \pi(r_{Bo}^2 - r_{Bi}^2) \quad (5)$$

where $\rho_w$ is the bed wall density, $c_{pw}$ is the bed wall heat capacity, J·mol$^{-1}$·K$^{-1}$; $A_w$ is the bed wall cross-sectional area, m$^2$; $r_{Bo}$ is the bed external radius, m; $r_{Bi}$ is the bed internal radius, m; $T_w$ is the wall temperature, $h_i$ is internal heat transfer coefficient, $h_o$ is the external heat transfer coefficient, and $T_{atm}$ is the ambient temperature.

**Linear Driving Force Mass Transfer Model.** The linear driving force (LDF) mass transfer model,[14−18] which is a tradition model, used to describe fixed-bed adsorption in this


dx.doi.org/10.1021/je201146r | J. Chem. Eng.Data 2012, 57, 568−576

work, is given below:

$$\frac{\partial q}{\partial t} = k(q^* - q) \tag{6}$$

where $q^*$ is the equilibrium adsorption capacity, g·(100 g)$^{-1}$.

For adsorption in the multicomponent organic gas, the extended Langmuir eq 7 is more appropriate than the isothermal adsorption equation.[10,19−22] The parameters of this equation are listed in Table 2.

**Table 2. Parameters of the Extended Langmuir Model**

| | | acetone | methylbenzene |
|---|---|---|---|
| $q_{max}$ | $aa$ | 34.579 | $9.53\cdot10^{-3}$ |
| | $bb$ | 601.043 | 2198.705 |
| $b_1$ | $cc_1$ | 819.633 | $8.75\cdot10^{-18}$ |
| | $dd_1$ | −1084.25 | 10987.49 |
| $b_2$ | $cc_2$ | $1.63\cdot10^{-13}$ | 812.413 |
| | $dd_2$ | 7323.171 | −1619.82 |

$$q_i = q_{\max,i}\frac{b_i C_i}{1 + \sum_j b_j C_j} \tag{7}$$

where $q_{max,i} = (aa_i/T^{1/2})\cdot e^{bb_i/T}$; $b_i = (cc_i/T^{1/2})\cdot e^{dd_i/T}$; $aa_i$, $bb_i$, $cc_i$, and $dd_i$ are the extension model fitting constants; and $C_i$ is the concentration of adsorbate.

**Coupled Diffusion Model.** Defining the Soret coefficient (thermal diffusion coefficient) as $L_s$, g·m$^{-1}$·s$^{-1}$·K$^{-1}$, and the Dufour coefficient (diffusion thermal coefficient) as $L_d$, W·m$^2$·g$^{-1}$, the mass and thermal flux from coupled heat and mass transfer is given below:

$$J_m = -L_s \text{ grad } T - \rho D \text{ grad } c_i \tag{8}$$

$$J_q = -\lambda \text{ grad } T - L_d \text{ grad } c_i \tag{9}$$

Using these equations, the coupled mass and energy equilibrium equation is given below:

$$-D_{ax}\frac{\partial^2 y_i}{\partial z^2} + v\frac{\partial y_i}{\partial z} - L_s\frac{\partial^2 T}{\partial z^2} + \frac{\partial y_i}{\partial t} + \rho_p\left(\frac{1-\varepsilon}{\varepsilon}\right)\frac{R_g T}{PM_i}\frac{\partial q_i}{\partial t} = 0 \tag{10}$$

$$-K_L\frac{\partial^2 T}{\partial z^2} - \varepsilon\rho L_d\frac{R_g T}{PM_i}\frac{\partial^2 y_i}{\partial z^2} + (\varepsilon\rho_g c_{pg} + \rho_p c_{ps})\frac{\partial T}{\partial t} - \varepsilon\lambda\frac{\partial^2 T}{\partial z^2} - \rho_p\sum_{i=1}^{n}(-\Delta H_i)\frac{\partial q_i}{\partial t} = 0 \tag{11}$$

The coupling of heat and mass transfer complicates theoretical calculations of the mass transfer coefficient, $k$, of LDF models; numerical simulation is the most commonly used method.

The physical parameters and its values of activated carbon in this model were mentioned in the literature,[10−12,17] and the values of the main parameters are listed in Table 3.

**Table 3. Mathematical Model Parameters**

| parameter | value |
|---|---|
| $\varepsilon$ | 0.5 |
| $D_{ax1}$/m$^2$·s$^{-1}$ | 0.057 |
| $D_{ax2}$/m$^2$·s$^{-1}$ | 0.0065 |
| $k_1$/m·s$^{-1}$ | 0.0055 |
| $k_2$/m·s$^{-1}$ | 0.0023 |
| $K_L$/W·m$^{-1}$·K$^{-1}$ | 0.00029 |
| $h_i$/W·m$^{-2}$·K$^{-1}$ | 0.016 |
| $h_o$/W·m$^{-2}$·K$^{-1}$ | 2.2 |
| $L$/m | 0.45 |
| $T$/K | 298.15 |
| $T_{atm}$/K | 298.15 |
| $v$/m·s$^{-1}$ | 0.3 |
| $R_p$/m | $3.16\cdot10^{-3}$ |
| $P$/kPa | 1.0 |

**Model Conditions.** The initial conditions of the model were the following:

$$C_i(z, 0) = 0, \qquad q_i(z, 0) = 0,$$

$$T(z, 0) = 298.15 \text{ K}, \qquad T_w(z, 0) = 298.15 \text{ K}$$

where $T$ is the gas temperature in the column and $T_w$ is the wall temperature.

The boundary conditions of the model were the following:

$$-D_L\left.\frac{\partial C_i}{\partial z}\right|_{z=0} = v(C_{i0} - C_{i,z=0}), \left.\frac{\partial C_i}{\partial z}\right|_{z=L} = 0$$

$$-K_L\left.\frac{\partial T}{\partial z}\right|_{z=0} = \rho_g C_{pg} v(T - T_{z=0}), \left.\frac{\partial T}{\partial z}\right|_{z=L} = 0$$

Owing to no deviation in results which are divided to more than 50 portions, to ensure simulation accuracy, the adsorption bed was divided into 50 consecutive sections. The reliability of the model and the convergence of simulation calculations can be determined by experimental verification.

## RESULTS AND DISCUSSION

**Distribution of Concentration and Temperature in Adsorption and Model Validation.** Some conditions were held constant or assumed to be constant in the experiments. For example, the temperature was 298.15 K; the air column gas velocity was 0.23 m·s$^{-1}$; and the concentration of acetone and methylbenzene was 0.84 g·m$^{-3}$ and 1.85 g·m$^{-3}$, respectively. Under these conditions, the discharge concentration and the variation in the adsorption temperature of acetone and methylbenzene were tested in a fixed adsorption bed.

The different times of the vapor phase concentration distribution of acetone and methylbenzene along the axis of the adsorption bed are shown in Figure 2. Initially, the intake gas concentration was the highest, and the discharge gas concentration was the lowest. During the adsorption process, the intake gas concentration decreased gradually, while the discharge gas concentration increased. Eventually, the concentration over the entire bed was similar to that of the inlet gas concentration.

Figure 3 shows the distribution of adsorption bed temperatures at different stages. The bed temperature was increased gradually from the gas intake to the outlet. The inlet temperature increased rapidly during the first adsorptive


dx.doi.org/10.1021/je201146r | J. Chem. Eng.Data 2012, 57, 568−576

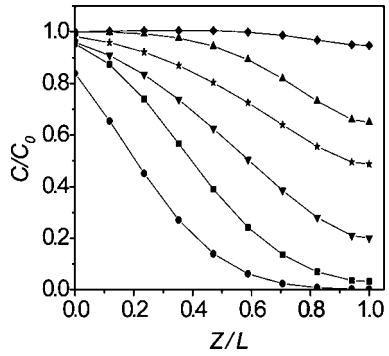


**Figure 2.** Gas concentration distribution. Acetone: ■, 1074 s; ▲, 3044 s; ♦, 6000 s; methylbenzene: ●, 1074 s; ▼, 3044 s; ★, 6000 s.

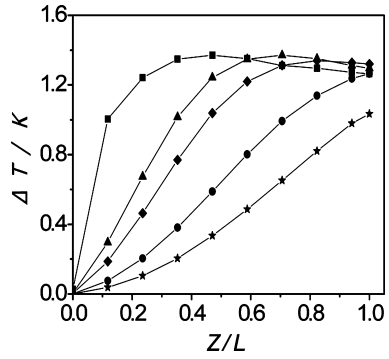


**Figure 3.** Temperature distribution of the adsorption bed. Symbols: ■, 70 s; ▲, 450 s; ♦, 650 s; ●, 1080 s; ★, 1550 s.

stage. In contrast, the outlet temperature increased gradually until a maximum temperature was reached.

Figure 4 shows that, for different experimental conditions, the simulated results agree well with the experimental results.

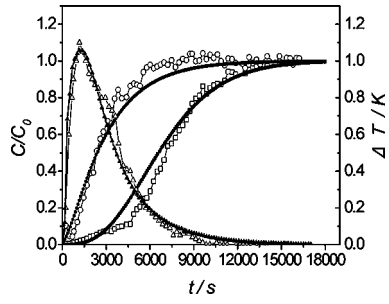


**Figure 4.** Curve of outlet temperature and gas concentration. Experimental: ○, acetone; □, methylbenzene; △, adsorption temperature; simulation: ●, acetone; ■, methylbenzene; ▲, adsorption temperature.

Thus, the model can be used for the prediction of results in the fixed-bed adsorption process.

**Effect of the Heat Transfer Coefficient on Adsorption.** The axial thermal conductivity coefficient ($K_L$), the internal heat transfer coefficient ($h_i$), and the external heat transfer coefficient ($h_o$) had little influence on the outlet gas concentration.

As shown in Figure 5, $C/C_0$, the outlet gas concentration of acetone and methylbenzene, remained below 0.001 as $K_L$ ranged from 0.000029 to 0.029, $h_i$ ranged from 0.0016 to 1.6, and $h_o$ ranged from 0.0022 to 2.2. According to the coupled equations, for the heat transfer coefficient to have a substantial impact on mass transfer, the temperature gradient must be large

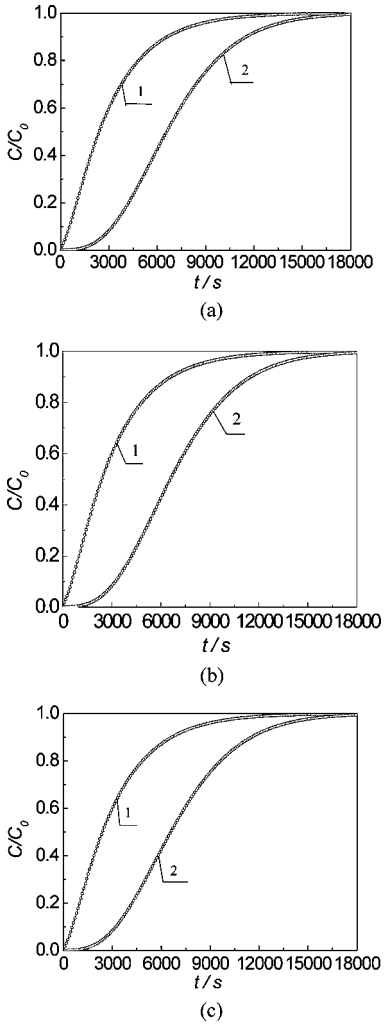


**Figure 5.** Effect of $K_L$ (a), $h_i$ (b), and $h_o$ (c) on outlet gas concentration. Symbols: 1, acetone; 2, methylbenzene; (a) □, $K_L$ = 0.000029; ○, $K_L$ = 0.00029; △, $K_L$ = 0.0029; ☆, $K_L$ = 0.029; (b) □, $h_i$ = 0.0016; ○, $h_i$ = 0.016; △, $h_i$ = 0.16; ☆, $h_i$ = 1.6; (c) □, $h_o$ = 0.0022; ○, $h_o$ = 0.022; △, $h_o$ = 0.22; ☆, $h_o$ = 2.2.

enough to affect thermal transfer. However, as the temperature gradient of the fixed-bed adsorption process is relatively small in this study, the influence on mass transfer is negligible.

The axial thermal conductivity coefficient ($K_L$) and the internal heat transfer coefficient ($h_i$) had a significant influence on the outlet gas temperature and temperature distribution, while the external heat transfer coefficient ($h_o$) did not obviously.

Different heat transfer coefficients impacted heat exchange in different beds position and thus affected outlet gas temperature and bed temperature distribution. As shown in Figures 6, increasing $K_L$ and $h_i$ decreased the peak outlet temperature, while increasing $h_o$ had not effect on the peak outlet temperature obviously. Thus, the three heat transfer coefficients affect heat transfer in the adsorption system differently.

In the fixed-bed adsorption process, gas contacted the adsorbent and then emitted heat. The peak outlet temperature decreased because, as $K_L$ and the axial transfer rate were increased, heat was released during adsorption. Conversely, as $h_i$ increased, heat transfer between the adsorbent and the bed wall increased until heat was fully exchanged, while heat transfer in the gas decreased quickly. This greatly reduced outlet gas


dx.doi.org/10.1021/je201146r | J. Chem. Eng.Data 2012, 57, 568−576

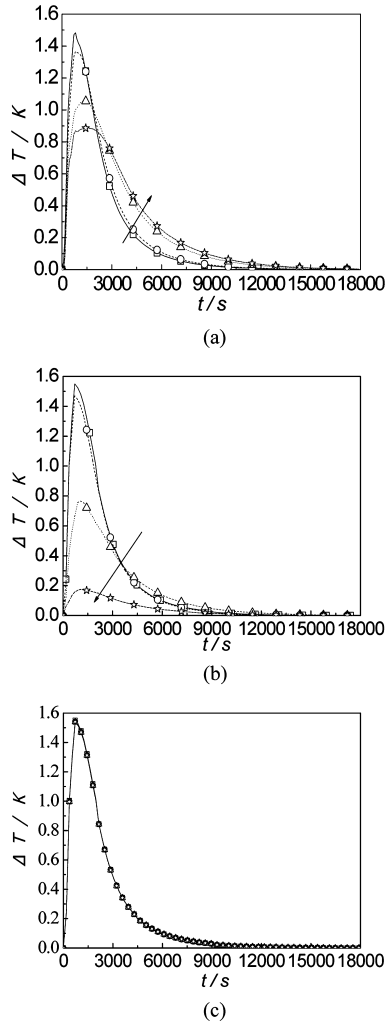


**Figure 6.** Effect of $K_L$ (a), $h_i$ (b), and $h_o$ (c) on outlet gas temperature. (a) □, $K_L$ = 0.00029; ○, $K_L$ = 0.0029; △, $K_L$ = 0.029; ☆, $K_L$ = 0.29; (b) □, $h_i$ = 0.0016; ○, $h_i$ = 0.016; △, $h_i$ = 0.16; ☆, $h_i$ = 1.6; (c) □, $h_o$ = 0.0022; ○, $h_o$ = 0.022; △, $h_o$ = 0.22; ☆, $h_o$ = 2.2.

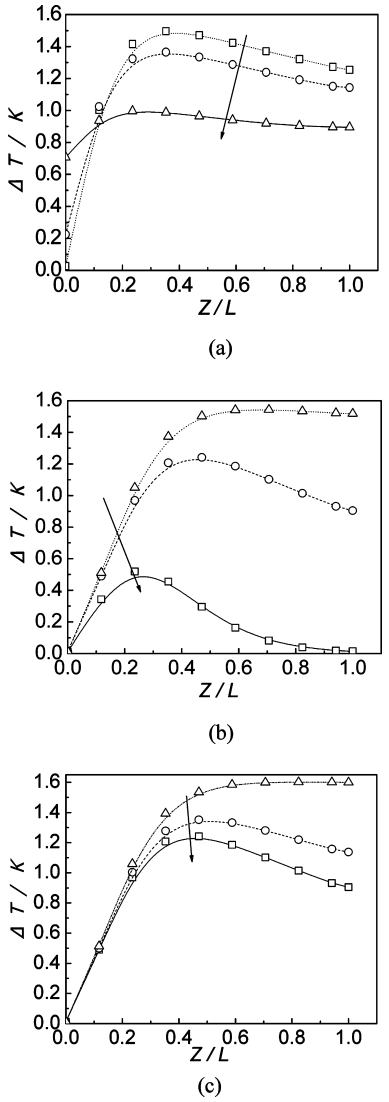


**Figure 7.** Effect of $K_L$ (a), $h_i$ (b), and $h_o$ (c) on temperature distribution. (a) □, $K_L$ = 0.0029; ○, $K_L$ = 0.029; △, $K_L$ = 0.29; (b) □, $h_i$ = 0.16; ○, $h_i$ = 0.016; △, $h_i$ = 0.0016; (c) □, $h_o$ = 0.22; ○, $h_o$ = 0.022; △, $h_o$ = 0.0022.

temperature. Although $h_o$ affected heat exchange between the bed wall and the external environment, it had no substantial impact on internal heat exchange in the adsorption system. Thus, changes in $h_o$ had an insignificant influence on the peak outlet gas temperature.

Changing the heat transfer coefficient of the adsorption system had two main effects. First, it altered the velocity of adsorption heat escaping to the environment. Second, it altered the velocity of internal heat equilibration. From Figure 7, as $K_L$ and the velocity of axial heat transfer increased, axial heat transfer came to equilibrium, and the velocity of heat escaping to the environment accelerated. Thus, the overall temperature distribution in the bed dropped and stabilized. Increasing $h_i$ and intensifying internal heat exchange quickly dispersed internal heat and lowered the overall temperature distribution in the bed. Moreover, increasing $h_o$ and the rate of heat exchange between the bed and the environment further lowered the temperature distribution, but the impact was smaller. Therefore, the degree of influence of the coefficients on adsorption system temperature is given as $h_i > K_L > h_o$.

**Effect of the Mass Transfer Coefficient on Adsorption.** Figures 8 and 9 show the axial diffusion coefficients of acetone ($D_{ax1}$) and methylbenzene ($D_{ax2}$) effect on outlet gas concentration and concentration distribution, respectively. From Figure 8, when the adsorption time was less than 4000 s, the outlet concentration of acetone increased with $D_{ax1}$ increasing. However, when the time was greater than 4000 s, the outlet concentration of acetone declined. The effect of $D_{ax2}$ on its outlet concentration was similar to that of acetone, but the inflection time for methylbenzene was around 8000 s. This can be explained by competition between axial mass transfer and adsorption. As the axial diffusion coefficient and the axial transmission velocity increased, the contact time between the adsorbate and the adsorbent decreased, and the outlet concentration was high. Prior to the inflection point, the saturation level of the adsorbent was the dominant factor. Larger axial diffusion coefficients reduced the early adsorption capacity and the saturation of the adsorbent. After the inflection point, adsorption was strong and the outlet concentration small.

As shown in Figure 9, the effect of the axial diffusion coefficient on the concentration distribution was similar to the effect on concentration. As the axial diffusion coefficient increased,


dx.doi.org/10.1021/je201146r | J. Chem. Eng.Data 2012, 57, 568−576

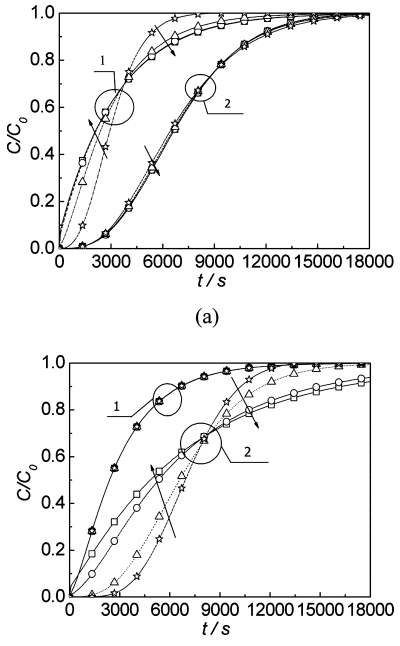


**Figure 8.** Effect of $D_{ax1}$ (a) and $D_{ax2}$ (b) on outlet gas concentration. Symbols: 1, acetone; 2, methylbenzene. (a) □, $D_{ax1}$ = 5.7; ○, $D_{ax1}$ = 0.57; △, $D_{ax1}$ = 0.057; ☆, $D_{ax1}$ = 0.0057; (b) □, $D_{ax2}$ = 0.65; ○, $D_{ax2}$ = 0.065; △, $D_{ax2}$ = 0.0065; ☆, $D_{ax2}$ = 0.00065.

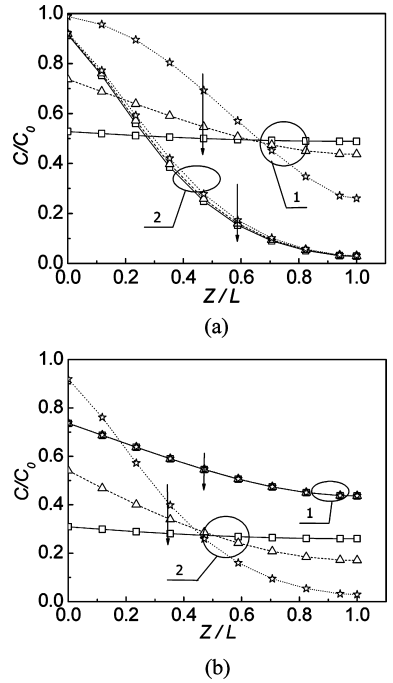


**Figure 9.** Effect of $D_{ax1}$ (a) and $D_{ax2}$ (b) on outlet gas concentration distribution. Symbols: 1, acetone; 2, methylbenzene. (a) □, $D_{ax1}$ = 0.57; △, $D_{ax1}$ = 0.057; ☆, $D_{ax1}$ = 0.0057; (b) □, $D_{ax2}$ = 0.65; △, $D_{ax2}$ = 0.065; ☆, $D_{ax2}$ = 0.0065.

the overall component concentration distribution tended to be smoothed.

The adsorption phase mass transfer coefficient of acetone ($k_1$) and methylbenzene ($k_2$) affected the outlet and bed concentration distributions at around 2060 s. As shown in Figure 10, each component of the adsorption phase mass

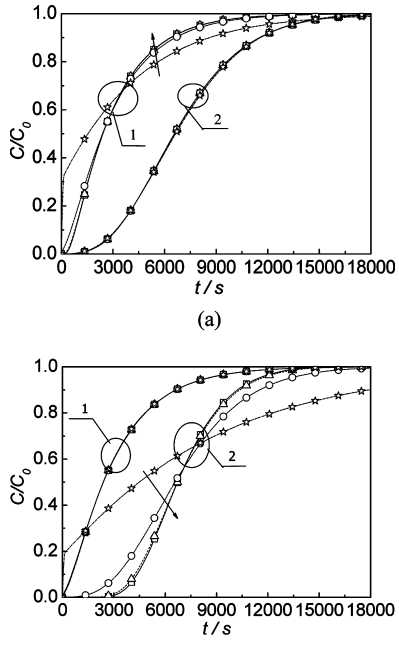


**Figure 10.** Effect of $k_1$ (a) and $k_2$ (b) on outlet gas concentration. Symbols: 1, acetone; 2, methylbenzene. (a) □, $k_1$ = 0.55; △, $k_1$ = 0.055; ○, $k_1$ = 0.0055; ☆, $k_1$ = 0.00055; (b) □, $k_2$ = 0.23; △, $k_2$ = 0.023; ○, $k_2$ = 0.0023; ☆, $k_2$ = 0.00023.

transfer coefficient only affected its outlet concentration and distribution. Adsorption competition was relatively minor because acetone and methylbenzene have similar molecular weights. Thus, the mass transfer coefficient affected the outlet concentration up to a critical point. In contrast to the axial diffusion coefficient, the outlet concentration decreased as the adsorption phase mass transfer coefficient increased. Prior to the critical point, the outlet concentration decreased as the adsorption phase coefficient increased, and after the critical point, the outlet concentration increased. This phenomenon reflects the different functions of the mass transfer coefficient and the axial diffusion coefficient. As the adsorption phase mass transfer coefficient and adsorbance increased, outlet concentration decreased. As the mass transfer coefficient and the degree of saturation of the adsorbent increased, adsorbance dropped in the later adsorption process, and the outlet concentration increased. Figure 11 shows the reduction in the bed concentration distribution of each component as the mass transfer coefficient increased. The coefficient $k_2$ had a significant influence on concentration distribution. Activated carbon has a higher capacity to adsorb methylbenzene than acetone, so changing the methylbenzene adsorption phase coefficient produced greater changes on its concentration distribution than did changing the acetone coefficient.

As shown in Figures 12 and 13, the axial diffusion coefficients ($D_{ax1}$, $D_{ax2}$) and the adsorption phase mass transfer coefficients ($k_1$, $k_2$) influenced the outlet temperature. From Figure 12, increasing $D_{ax1}$ increased the outlet gas temperature before about 2500 s, then the temperature was decreased by $D_{ax1}$ increasing from 2500 s to about 6000 s. But after this critical point about 6000 s, increasing $D_{ax1}$ increased the outlet gas temperature slightly until stability. For $D_{ax2}$, the critical point was nearly 3200 s. After this point, the outlet gas temperature was also decreased by $D_{ax2}$ increasing. Figure 13 shown that


dx.doi.org/10.1021/je201146r | J. Chem. Eng.Data 2012, 57, 568−576

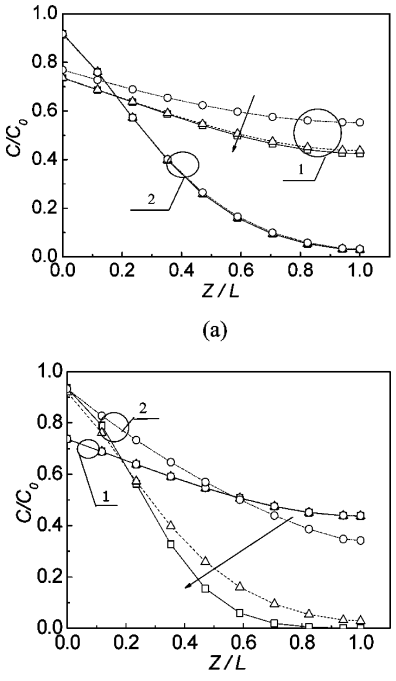


**Figure 11.** Effect of $k_1$ (a) and $k_2$ (b) on outlet gas concentration distribution. Symbols: 1, acetone; 2, methylbenzene. (a) □, $k_1$ = 0.055; △, $k_1$ = 0.0055; ○, $k_1$ = 0.00055; (b) □, $k_2$ = 0.023; △, $k_2$ = 0.0023; ○, $k_2$ = 0.00023.

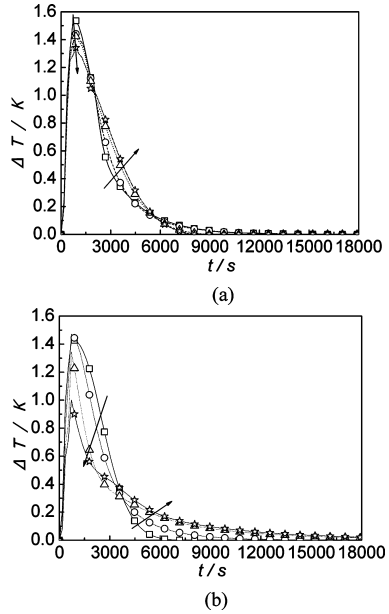


**Figure 12.** Effect of $D_{ax1}$ (a) and $D_{ax2}$ (b) on outlet gas temperature. (a) □, $D_{ax1}$ = 0.0057; ○, $D_{ax1}$ = 0.057; △, $D_{ax1}$ = 0.57; ☆, $D_{ax1}$ = 5.7; (b) □, $D_{ax2}$ = 0.00065; ○, $D_{ax2}$ = 0.0065; △, $D_{ax2}$ = 0.065; ☆, $D_{ax2}$ = 0.65.

increasing $k$ increased outlet temperatures. The mass transfer coefficient influenced temperature mainly by altering adsorbance and the release of adsorption heat. Increasing the axial diffusion coefficient shortened the contact time between the adsorbate and the adsorbent and decreased adsorbance, the release of adsorption heat, and the peak outlet temperature. Conversely, increasing $k$ increased adsorbance, the release of adsorption heat, and the peak outlet temperature.

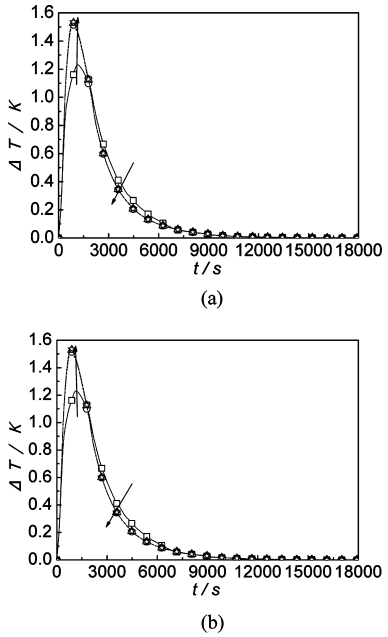


**Figure 13.** Effect of $k_1$ (a) and $k_2$ (b) on outlet gas temperature. (a) □, $k_1$ = 0.00055; ○, $k_1$ = 0.0055; △, $k_1$ = 0.055; ☆, $k_1$ = 0.55; (b) □, $k_2$ = 0.00023; ○, $k_2$ = 0.0023; △, $k_2$ = 0.023; ☆, $k_2$ = 0.23.

**Coupled Diffusion Effect of Heat and Mass Transfer on Adsorption.** The influence of the Soret coefficient ($L_s$) on the outlet gas concentration of acetone and methylbenzene and the concentration distribution in the adsorption bed at different times is shown in Figure 14.

The outlet concentration of acetone and methylbenzene was influenced by $L_s$, and as $L_s$ increased, the concentration distribution of each component decreased. Figure 15 shows the influence of the Dufour coefficient ($L_d$) on heat transfer in adsorption. As shown in this figure, $L_d$ did not clearly influence outlet temperature or bed temperature distribution.

In the presence of coupling effects, mass flux is driven by temperature differences in the adsorption system, which can change the original concentration. In contrast, thermal flux is driven by differences in concentration, which can change the temperature in the system.

Gradients in both concentration and temperature produce cross-coupled heat and mass transfer. From the coupled equations, the mass equilibrium equation had a temperature gradient, and the energy conservation equation had a concentration gradient. Experimental results matched this model well, so we deduce that the cross-coupled effect of mass and heat transfer impacts the adsorption process. Li et al.[23] found that, with high inlet velocity and temperature (>1000 K) in porous media, the Soret and Dufour effects were not negligible. In this study, the Soret and Dufour effects were not obvious because of low inlet gas concentration and low internal gas velocity.

However, based on our simulation results, the temperature gradient does influence mass transfer. The gradual increase of the Soret coefficient produced a negative concentration gradient and thus changed the bed concentration distribution and the outlet concentration. Stated more simply, temperature differences affect mass transfer more than concentration differences affect heat transfer. Therefore, heat transfer caused by concentration differences could be neglected in adsorption processes.


dx.doi.org/10.1021/je201146r | J. Chem. Eng.Data 2012, 57, 568−576

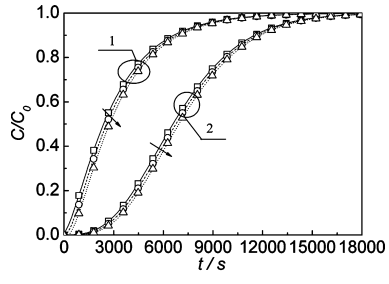


(a)

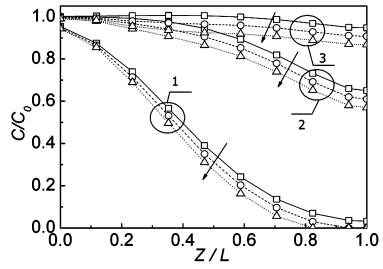


(b)

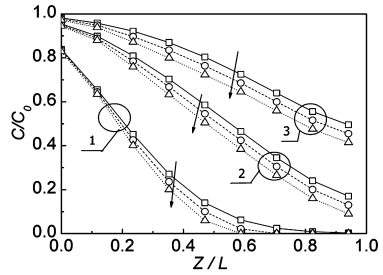


(c)

**Figure 14.** Effect of $L_s$ on outlet gas concentration (a) and the concentration distribution of acetone (b) and methylbenzene (c). Symbols: □, $L_s$ = 0.00002; ○, $L_s$ = 0.0002; △, $L_s$ = 0.002. (a) 1, acetone; 2, methylbenzene; (b) 1, 1074 s; 2, 3044 s; 3, 6000 s; (c): 1, 1074 s; 2, 3044 s; 3, 6000 s.

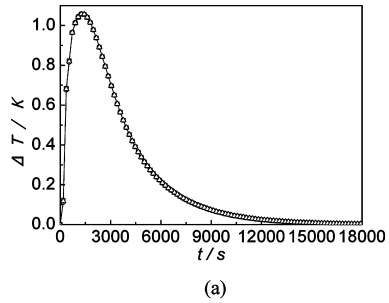


(a)

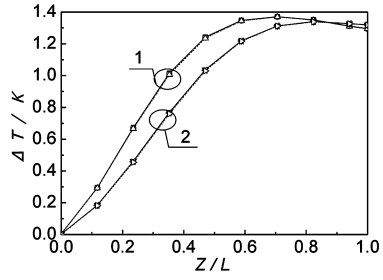


(b)

**Figure 15.** Effect of $L_d$ on outlet temperature (a) and temperature distribution (b). Symbols: □, $L_d$ = 0.00005; ○, $L_d$ = 0.0005; △, $L_d$ = 0.005. (b) 1, 450 s; 2, 650 s.

## CONCLUSIONS

By comparing adsorption experiments with numerical simulation results, the coupled diffusion model of heat and mass transfer in a fixed-bed adsorption process was presented. The coupled effects of heat and mass transfer on the adsorption process was studied, and the impact of coefficients on adsorption was discussed. The results from numerical simulations support the following conclusions:

(1) The simulation results agreed well with experimental results and validated the model based on experimental data for fixed-bed adsorption.

(2) Variation of the heat transfer coefficients has little effect on mass transfer. The rank of the effect of the coefficients on the temperature gradient is as follows: internal heat transfer coefficient > axial thermal conductivity coefficient > external heat transfer coefficient.

(3) Heat transfer coefficients have little effect on mass transfer. In contrast, mass transfer coefficients have some impact on heat transfer.

(4) The mass transfer effects caused by a temperature gradient are more obvious than heat transfer effects caused by a concentration gradient.

## AUTHOR INFORMATION

### Corresponding Author

*Tel.: +86-0731-88877195. Fax: +86-0731-88879863. E-mail: liqingli@hotmail.com.

### Funding

This work is financed by the National Natural Science Foundation of China (Nos. 20976200 and 20676154).

## ACKNOWLEDGMENTS

We are grateful to all of the reviewers, whose comments and suggestions have significantly improved the quality of this manuscript.

## REFERENCES

(1) Popescu, M.; Joly, J. P.; Carré, J.; Danatoiu, C. Dynamical adsorption and temperature-programmed desorption of VOCs (toluene, butyl acetate and butanol) on activated carbons. *Carbon* **2003**, *41*, 739−748.

(2) Fuertes, A. B.; Marbán, G.; Nevskaia, D. M. Adsorption of volatile organic compounds by means of activated carbon fibre-based monoliths. *Carbon* **2003**, *41*, 87−96.

(3) Lillo-Ródenas, M. A.; Fletcher, A. J.; Thomas, K. M.; Cazorla-Amorós, D.; Linares-Solano, A. Competitive adsorption of a benzene-toluene mixture on activated carbons at low concentration. *Carbon* **2006**, *44*, 1455−1463.

(4) Romero-Anaya, A. J.; Lillo-Ródenas, M. A.; Linares-Solano, A. Spherical activated carbons for low concentration toluene adsorption. *Carbon* **2010**, *48*, 2625−2633.

(5) Martynenko, O. G.; Pavlyukevich, N. V. Heat and mass transfer in porous media. *J. Eng. Phys. Thermophys.* **1998**, *71*, 1−13.

(6) Malashetty, M. S.; Gaikwad, S. N. Effect of cross diffusion on double diffusive convection in the presence of horizontal gradients. *Int. J. Eng. Sci.* **2002**, *40*, 773−787.

(7) Cheng, C. Y. Soret and Dufour effects on heat and mass transfer by natural convection from a vertical truncated cone in a fluid-saturated porous medium with variable wall temperature and concentration. *Int. Commun. Heat Mass Transfer* **2010**, *37*, 1031−1035.

(8) Postelnicu, A. Influence of chemical reaction on heat and mass transfer by natural convection from vertical surface in porous media considering Soret and Dufour effects. *Heat Mass Transfer* **2007**, *43*, 595−602.

(9) Coelho, R. M. L.; Telles, A. S. Extended Graetz problem accompanied by Dufour and Soret effects. *Int. J. Heat Mass Transfer* **2002**, *45*, 3101−3110.
(10) Li, L. Q. *Theoretical and Experimental Study on the Treatment of Organic Vapors by Adsorption and Pressure Swing Adsorption (PSA)*. Ph.D. thesis. Hunan University, Changsha, China, 2004.
(11) Ruthven, D. M. *Principles of Adsorption and Adsorption Processes*; Wiley-Interscience Publications: Toronto, Canada, 1984.
(12) Serbezov, A.; Sotirchos, S. V. Mathematical modeling of multicomponent nonisothermal adsorption in sorbent particles under pressure swing conditions. *Adsorption* **1998**, *4*, 93−111.
(13) Yang, R. T. *Gas Separation by Adsorption Processes*; Butterworth Publishers: Waltham, MA, 1986.
(14) Jensen, C. R. C.; Seaton, N. A.; Gusev, V.; O'Brien, J. A. Prediction of multicomponent adsorption equilibrium using a new model of adsorbed phase nonuniformity. *Langmuir* **1997**, *13*, 1205−1210.
(15) Li, L. Q.; Liu, Z.; Qin, Y. X.; Sun, Z.; Song, J. F.; Tang, L. Estimation of volatile organic compound mass transfer coefficients in the vacuum desorption of acetone from activated carbon. *J. Chem. Eng. Data* **2010**, *55*, 4732−4740.
(16) Leinekugel-Le-Cocq, D.; Tayakout-Fayolle, M.; Gorrec, Y. L.; Jallut, C. A double linear driving force approximation for non-isothermal mass transfer modeling through bi-disperse adsorbents. *Chem. Eng. Sci.* **2007**, *62*, 4040−4053.
(17) Sircar, S. Gas sorption kinetics by differential closed-loop recycle method: Effect of heat of adsorption. *Adsorption* **2006**, *12*, 259−266.
(18) Sircar, S.; Hufton, J. R. Why does the linear driving force model for adsorption kinetics work? *Adsorption* **2000**, *6*, 137−147.
(19) Rao, M. B.; Sircar, S. Thermodynamic consistency for binary gas adsorption equilibria. *Langmuir* **1999**, *15*, 7258−7267.
(20) Li, L. Q.; Zhu, Z. S.; Qin, Y. X.; Song, J. F.; Liu, X. Y. Simulation on isotherm adsorption of two-component organic gas and heat and mass transfer analysis. *Proc. Chin. Soc. Elec. Eng.* **2008**, *28*, 46−52.
(21) He, Y. F.; Yun, J. H.; Seaton, N. A. Adsorption equilibrium of binary methane/ethane mixtures in BPL activated carbon: Isotherms and calorimetric heats of adsorption. *Langmuir* **2004**, *20*, 6668−6678.
(22) Do, D. D. *Adsorption Analysis: Equilibria and Kinetics*; Imperial College Press: London, 1998.
(23) Li, M. C.; Tian, Y. W.; Zhai, Y. C. Soret and Dufour effects in strongly endothermic chemical reaction system of porous media. *Trans. Nonferrous Met. Soc. China* **2006**, *16*, 1200−1204.